

See discussions, stats, and author profiles for this publication at: <https://www.researchgate.net/publication/51244114>

DFT Study on the Radical Anions Formed by Primaquine and Its Derivatives

ARTICLE *in* CHEMICAL RESEARCH IN TOXICOLOGY · JUNE 2011

Impact Factor: 3.53 · DOI: 10.1021/tx200094v · Source: PubMed

CITATIONS

7

READS

26

3 AUTHORS, INCLUDING:



Larry A Walker

University of Mississippi

263 PUBLICATIONS 3,422 CITATIONS

SEE PROFILE



Robert J Doerksen

University of Mississippi

84 PUBLICATIONS 2,749 CITATIONS

SEE PROFILE

Published in final edited form as:

Chem Res Toxicol. 2011 September 19; 24(9): 1476–1485. doi:10.1021/tx200094v.

DFT Study on the Radical Anions Formed by Primaquine and Its Derivatives

Haining Liu[†], Larry A. Walker^{‡,§}, and Robert J. Doerksen[†]

Robert J. Doerksen: rjd@olemiss.edu

[†]Department of Medicinal Chemistry, School of Pharmacy, University of Mississippi, University MS, 38677

[‡]Department of Pharmacology, School of Pharmacy, University of Mississippi, University MS, 38677

[§]Department of National Center for Natural Products Research, School of Pharmacy, University of Mississippi, University MS, 38677

Abstract

The electron affinities (EA) of the 8-aminoquinoline antimalarial drug primaquine and several of its metabolites were studied using the density functional theory method. We first considered six substituents at the 5-position, $-\text{CH}_3$, $-\text{OH}$, $-\text{OCH}_3$, $-\text{Ph}$, $-\text{OPh}$ and $-\text{CHO}$. We found that in the gas phase the adiabatic EAs are similar to that of the parent primaquine for the $-\text{CH}_3$, $-\text{OH}$ and $-\text{OCH}_3$ substituents. In contrast, the $-\text{Ph}$, $-\text{OPh}$ and $-\text{CHO}$ substituents all markedly increase the adiabatic EA. However, only the $-\text{CHO}$ substituted compound is predicted to form a stable covalently bound radical anion in the gas phase due to its significant positive vertical EA relative to that of the parent primaquine. In addition, when the 8-position is substituted by the *N*-hydroxyl group or a quinone-imine structure is formed, the electron capture ability is significantly increased. In aqueous solution, all these molecules have significantly larger adiabatic EAs than in the gas phase. In addition, all the vertical EAs are positive in aqueous solution. The implications of these findings for contributing to our mechanistic understanding of the red cell toxicity of 8-aminoquinoline compounds are further discussed.

1. Introduction

It is of fundamental importance to determine the electron affinities of atoms and molecules, as this helps for understanding of their properties and the chemical processes in which they participate. In biological systems, certain cofactors, such as flavin adenine dinucleotide (FAD) and nicotinamide adenine dinucleotide (NAD^+), are known to be able to accept and transfer electrons.¹ Their function is crucial to redox enzymatic reactions. In addition, electron attachment to a biomolecule may initiate the damage of biomacromolecules. For example, DNA is able to capture electrons,²⁻⁵ which further causes lesions such as strand breaks,⁶⁻¹⁰ base pair mutations^{11,12} and glycosidic bond cleavage.¹³⁻¹⁵ Hence, there is a considerable interest in studying the ability of a neutral molecule to capture an electron and the properties of the formed radical anions. Such studies could be useful for predicting and understanding drug mechanisms of action and how toxicities can arise.

Correspondence to: Robert J. Doerksen, rjd@olemiss.edu.

Supporting Information Available: The optimized geometries and relevant energies of all the structures considered in this study. This material is available free of charge via the Internet at <http://pubs.acs.org>.

We are particularly interested in the 8-aminoquinoline (8-AQ) molecules, which are an important class of antimalarial drugs. The only 8-AQ now clinically used for radical cure of relapsing malaria is primaquine (PQ). *In vivo*, PQ forms a number of metabolites (Figure 1). For example, a substantial fraction of the drug is transformed to carboxyprimaquine by amine oxidases and aldehyde dehydrogenase.^{16,17} In addition, a small fraction is metabolized by the cytochrome P450 enzymes to form hydroxylated metabolites, including 5-hydroxyprimaquine (5-HPQ),^{18,19} 5,6-dihydroxyprimaquine (5,6-HPQ),²⁰ and 6-methoxy-8-(*N*-hydroxy)aminoquinoline (MAQ-NOH).^{21,22} However, a serious drawback of the use of PQ is that several of its metabolites are able to induce oxidative damage in target cells; among the most serious reactions is the susceptibility of subjects deficient in erythrocytic glucose-6-phosphate dehydrogenase (G6PD) to red cell oxidative stress and subsequent hemolysis.²³⁻²⁵ The hallmark features of these PQ metabolites (or other redox-linked species) in red cells are the conversion of hemoglobin to methemoglobin by oxidizing iron from the ferrous form to the ferric form and the generation of reactive oxygen species, such as the superoxide radical and hydrogen peroxide. Unfortunately, the precise chemical mechanism of methemoglobinemia caused by PQ is still not clear.^{23,25} Recently, we proposed a mechanism that can be used to explain the methemoglobinemia caused by PQ metabolites. Our docking and density functional theory (DFT) calculations²⁶ show that the PQ metabolite 5-HPQ is able to facilitate the conversion of O₂ to H₂O₂ by donating an electron to the Fe-O₂ moiety. In the meantime, Fe(II) is converted to Fe(III), hence causing the formation of methemoglobin. However, another possible mechanism is that a PQ metabolite acts as an electron acceptor by directly abstracting an electron from Fe(II), which causes the conversion of hemoglobin to methemoglobin. Therefore, determination of the electron affinities of PQ and its metabolites will be able to provide insight into the feasibility of this mechanism, which will further aid our understanding of the origins of the toxicity caused by PQ and related antimalarial drugs.

Compared to experimental techniques, theoretical calculations offer an alternative and inexpensive method to obtain electron affinities. Recently, Schaefer's carefully calibrated B3LYP/DZP++ method has been found to be able to provide accurate electron affinities with average errors <0.12 eV²⁷ and has been widely used for biomolecules.^{3,5,15,28-35} In the present study, a systematic analysis was performed on the electron affinities of PQ and several of its derivatives.

2. Computational Methods

All calculations were performed using the Gaussian 09 program.³⁶ Geometries were optimized using the B3LYP³⁷⁻³⁹ method in conjunction with the DZP++ basis set. The construction of this basis set can be found in ref. 27. Frequency calculations were performed to confirm that all the optimized structures correspond to minima on the potential energy surface and to obtain zero-point vibrational energies (ZPVE), which were used as energy corrections when appropriate. In order to consider the effect of a polar environment, single point calculations were performed using the integral equation formalism polarizable continuum model (IEFPCM) based on the optimized gas-phase geometries. For selected molecules, geometries were also optimized using the IEFPCM method. A dielectric constant (ϵ) of 78.36 was used to model aqueous solution.

Electron affinities were calculated according to the following definitions:

$$\text{Adiabatic electron affinity (AEA)} = E(\text{optimized neutral}) - E(\text{optimized anion})$$

$$\text{Vertical electron affinity (VEA)} = E(\text{optimized neutral}) - E(\text{anion at optimized neutral geometry})$$

$$\text{Vertical detachment energy (VDE)} = E(\text{neutral at optimized anion geometry}) - E(\text{optimized anion})$$

3. Results and Discussion

Effects of substituents at the 5-position

We started with several model molecules, in which the long alkyl group connected to the 8-amino group of PQ is replaced by a methyl. Six substituents, $-\text{CH}_3$ (**2**), $-\text{OH}$ (**3**), $-\text{OCH}_3$ (**4**), $-\text{Ph}$ (**5**), $-\text{OPh}$ (**6**) and $-\text{CHO}$ (**7**), were chosen in this work. All the optimized geometries are provided in the Supporting Information. The key structural parameters and calculated AEAs, VEAs and VDEs are listed in Tables 1 and 2, respectively.

Upon electron attachment, the most obvious structural changes were observed on the exocyclic groups. For example, the C8–N11 bond significantly lengthens by 0.04–0.06 Å (Table 1). The N11–C12 bond also correspondingly slightly lengthens by 0.01–0.02 Å. In addition, the terminal methyl connected to the 8-amino group largely deviates from the quinoline plane (cf. the C8'–C8–N11–C12 dihedral angle in Table 1). Furthermore, it should be noted that in **1–4** and **6** the C5–R bond (R refers to the exocyclic atom directly connected to C5) stays the same or slightly lengthens by 0.02 Å upon electron attachment. In contrast, this bond shortens by 0.02 and 0.03 Å in **5** and **7**, respectively. This may be due in part to better electron delocalization ability of the $-\text{Ph}$ and $-\text{CHO}$ moiety in the radical anion of **5** and **7** (see Figure 2), which makes the C5–R bonds shorter.

All the molecules have positive AEA (Table 2), indicating that they have a tendency to accept an additional electron. The AEAs of **1–4** are very similar, suggesting that the $-\text{CH}_3$, $-\text{OH}$ and $-\text{OCH}_3$ substituents at the 5-position do not have significant effects on AEA. In contrast, the $-\text{Ph}$, $-\text{OPh}$ and $-\text{CHO}$ substituents are all able to increase the AEA significantly. **7**, with the electron-withdrawing group $-\text{CHO}$ at the 5-position, has the largest AEA. As for the VEAs and VDEs, they are all quite different from the AEAs due to the considerable changes in geometry between the neutral and radical anion molecules. The VEAs of **1–6** are negative, suggesting that upon initial electron attachment these ‘vertically’ formed anions lie higher in energy than the neutral molecules. Thus, in the gas phase these anions may not have sufficient lifetime to relax to form stable covalently bound anions. In contrast, **7** has a positive VEA, further indicating that it is most ready to capture an electron. Its large VDE also suggests that once the radical anion is formed, it should have a long enough lifetime to be involved in other reactions.

In order to find the location of the excess electron, the singly occupied molecular orbitals (SOMO) of the electronically stable radical anions (Figure 2) and the vertically-attached electron anions (Figure 3) were studied. Similar approaches to distinguish valence-bound and dipole-bound anions have been used previously in the literature.^{3,4,6,40,41} Except for **3**, the vertically-attached electron anion species do not show significant dipole-bound character. Furthermore, in both the electronically stable radical anions and the vertically-attached electron anions, the excess electron is primarily delocalized over the quinoline ring and the 8-amino group. In addition, a very small fraction of the electron is also delocalized over the substituent at the 5-position in **2–4** and **6**. In contrast, a much more significant portion of the electron is found to be delocalized at the 5-position substituents in **5** and **7**. This is probably due to the better electron delocalization ability of the phenyl and formyl groups.

Effects of the alkyl-amine chain at the 8-position

We then included the complete alkyl-amine chain $-\text{CH}(\text{CH}_3)\text{CH}_2\text{CH}_2\text{CH}_2\text{NH}_2$ at the 8-position in order to investigate its effects. Again, six substituents, $-\text{CH}_3$ (**9**), $-\text{OH}$ (**10**),

–OCH₃ (**11**), –Ph (**12**), –OPh (**13**) and –CHO (**14**), were selected. The stereocenter at C12 (see Table 3) was chosen in the *S* configuration. The calculated AEAs, VEAs and VDEs, and key structural parameters are listed in Tables 2 and 3, respectively.

The alkyl chain that is connected to the 8-amino group does not have a significant effect on the bond lengths. For both neutral and anion molecules, the changes in the bond lengths compared to having only a methyl connected to the 8-amino group are <0.02 Å. Similarly, the C8–N11 bond is lengthened by 0.03–0.07 Å upon electron attachment. In addition, compared to the model molecules, a similar trend in the changes of the C5–R bond length between neutral and anion molecules is observed. That is, the C5–R bond shortens in the –Ph and –CHO substituted derivatives (**12** and **14**), while it slightly lengthens or stays the same in the rest of the molecules (**8–11** and **13**). Furthermore, C12 is also observed to deviate from the quinoline plane in the anions as shown by the C8'–C8–N11–C12 dihedral angle. However, compared to the above model 8-AQ molecules with only a methyl group at the 8-position the differences of the C8'–C8–N11–C12 dihedral angle between neutral and anion molecules are now much less significant. This thus suggests that the alkyl chain at the 8-position has a role of limiting the structural changes that occur upon electron attachment.

As for the electron affinities (Table 2), the AEAs of **8–14** are again all positive. However, they only marginally decrease by 0.02 eV or increase by maximally 0.03 eV compared to those of **1–7**, indicating that the terminal alkyl chain does not significantly affect the adiabatic electron capture ability. In contrast, the VEAs of **8–13**, but not of **14**, significantly increase by 0.08–0.18 eV, while the VDEs decrease by 0.06–0.10 eV. This is likely due to the smaller structural changes between neutral and anion molecules upon inclusion of the alkyl chain. Although the VEAs of **8–13** increase compared with their counterparts **1–6**, they are still negative or only slightly positive. Thus, the 'vertically' formed anions may not have sufficient lifetimes to relax to form stable covalently bound anions. Only when the 5-position is substituted by a strong electron-withdrawing group, such as –CHO, can the PQ-based compounds form covalently stable radical anions upon accepting an electron.

The SOMOs of **8–14** in the electronically stable radical anions and vertically-attached electron anions are shown in Figures 4 and 5, respectively. In the electronically stable anions, the excess electron is still primarily delocalized on the quinoline ring and the amino group at the 8-position. This may explain the small change of AEA for **8–14** relative to their **1–7** counterparts. The long alkyl group does not carry significant electron density except that a small fraction is found on the terminal –NH₂ group. In contrast, except for **14** the vertically-attached electron anions show significant dipole-bound character around the terminal –NH₂ group. This feature is observed to diminish in **14**, which may explain its positive VEA.

Electron affinity of other possible metabolites

In addition to the above modifications at the 5-position, a number of other 8-AQ metabolites can also be formed. For example, the long alkyl group at the 8-position can be removed to form 6-methoxy-8-aminoquinoline (MAQ, **15**).^{21,22} In addition, one of the amine hydrogens of MAQ can be further substituted with a hydroxyl group to form MAQ-NOH (**16**). Furthermore, a quinone-imine intermediate (**17**) was thought to be involved in the metabolism of 8-AQ drugs.⁴² Therefore we also considered in this work the ability of these additional molecules (Figure 6) to capture an electron.

Upon electron attachment, a lengthening of the C8–N11 (see Figure 6) bond is again observed, from 1.37 Å to 1.42 Å, 1.40 Å to 1.43 Å and 1.29 Å to 1.33 Å in **15**, **16** and **17**, respectively. In addition, the N11–O12 and C5–O5' bonds in **16** and **17** are also lengthened from 1.43 Å to 1.46 Å and 1.23 Å to 1.27 Å, respectively.

Table 4 lists the calculated AEAs, VEAs and VDEs of **15**–**17**, while the SOMOs of the electronically stable anions and vertically-attached electron anions are shown in Figures 7 and 8, respectively. Compared with **8**, the AEA slightly increases by 0.05 eV when the 8-position is substituted with an $-\text{NH}_2$ group (**15**). In addition, its VEA is also negative (−0.11 eV), due in part to the significant dipole-bound character in the vertically-attached electron anion (Figure 8). However, when one of the amine hydrogens is replaced with a hydroxyl group to form **16**, the AEA significantly increases to 0.56 eV. This is likely due to the fact that the $-\text{OH}$ group helps to delocalize the excess electron in the radical anion, as can be seen from its SOMO surface (Figure 7). In addition, the VEA of **16** is positive (0.23 eV) with no significant dipole-bound character observed in its ‘vertically’ formed anion (Figure 8), further suggesting that this ‘vertically’ formed anion should be relatively stable and have a long enough lifetime to further relax and form a stable covalently bound anion. The quinone-imine derivative, **17**, has an AEA which is further increased to 1.63 eV. In addition, its VEA is also quite high at 1.28 eV. They both suggest that **17** should easily be able to form a stable radical anion. Furthermore, it should also be noted that the SOMO of **17** is different from those of all the other molecules. In **17**, the unhybridized p orbitals of O5' and N11 contribute significantly to the SOMO (Figure 7). However, similar orbitals do not exist in the other molecules, since they lack the C5=O5' and C8=N11 double bonds found in **17**.

We further considered two other derivatives, **18** and **19** (Figure 4). The former corresponds to the addition of the alkyl chain at the 8-amino group to **16**, while the latter corresponds to the removal from **17** of the alkyl chain at the 8-amino group. Their calculated AEAs, VEAs and VDEs are listed in Table 4. The high AEAs and positive VEAs indicate that **18** and **19** should also be able to form stable radical anions. In addition, all the AEAs, VEAs and VDEs are slightly reduced upon inclusion of the long alkyl chain.

The effects of solvation

In order to consider solvation effects, we first calculated the AEAs, VEAs and VDEs of **1** and **8** in aqueous solution using two approaches: (i) single point calculations in solution based on the optimized gas phase geometries, and (ii) geometry optimizations in solution. As shown in Table 5, no significant differences were observed using these two approaches. The AEAs and VEAs differed by only 0.01 eV, while slightly larger differences of 0.03 and 0.09 eV were found for the VDEs of **1** and **8**, respectively. Hence, it is reasonable to use the optimized gas phase geometries for calculating the electron affinities in solution. Therefore, all other solution phase electron affinities were calculated with this approach.

It can be seen from Tables 5 and 6 that the inclusion of solvation significantly increases the gas phase electron affinities. However, the general trend of AEA observed in the gas phase remains the same in solution. For example, the exocyclic $-\text{CH}_3$, $-\text{OH}$ and $-\text{OCH}_3$ substituents at the 5-position do not have a significant effect on AEA compared with that of the parent primaquine. In addition, the electron-withdrawing substituent $-\text{CHO}$ results in the largest AEA among **1**–**14**. However, it should be noted that in solution the AEA of the $-\text{Ph}$ substituted derivative (**5**) is essentially the same as that of PQ. In contrast, in the gas phase **5** has a markedly larger AEA than that of PQ. In solution phase the quinone-imine derivatives (**17** and **19**) were again found to have the largest AEAs among all the molecules considered in this study.

All the VEAs are positive in solution. Hence, all these molecules should be able to form stable radical anions in biological systems. In addition, the differences between AEAs and VEAs are consistently ~ 0.3 eV. This suggests that the formed radical anions should be valence-bound since the energy difference of 0.3 eV is approximately the expected amount of relaxation energy for a valence-bound anion.^{40,43} This is further demonstrated in the

SOMOs of selected vertically-attached anions which showed dipole-bound character in the gas phase (Figure 9). As can be seen, aqueous solution indeed changes these anions from dipole-bound to valence-bound, hence resulting in positive VEAs. Furthermore, the positive VDEs of all the molecules indicate that electron auto-detachment is not expected to occur on these anions in water.

Implications for the toxicity of 8-AQ drugs

Elucidation of the electron transfer process is important for understanding of the methemoglobinemia caused by 8-AQ drugs. It is apparent that Fe(II) must lose an electron to be converted to Fe(III). However, the acceptor of this electron is not clear. In our previous study using 5-HPQ as a model compound for 8-AQ,²⁶ we found that O₂ is able to accept this electron as well as another electron from 5-HPQ as it is converted to H₂O₂. In addition to this mechanism, another possible electron acceptor for Fe(II) is the 8-AQ itself and/or its metabolites. It is thought that PQ, which does not show toxicity, needs metabolic activation to cause methemoglobinemia.⁴² One example of a toxic metabolite is 5-HPQ.²³ However, it is found in the present study that 5-HPQ (**10**) has essentially the same AEA as the parent PQ (**8**) in solution. Hence, the toxicity of 5-HPQ cannot be explained by the mechanism that Fe(II) *directly* transfers an electron to it. There must be other species that accept this electron in the methemoglobin-forming process. Our previous study,²⁶ which identified O₂ as this electron acceptor, appears to provide a more feasible mechanism.

Several approaches to make 8-AQ's even better electron acceptors have been found in the present study. These include the use of electron-withdrawing groups at the 5-position, the addition of an *N*-hydroxyl group at the 8-position and the conversion to the quinone-imine derivative. Among these species, the *N*-hydroxyl^{21,22} and quinone-imine⁴⁴ metabolite are known to be able to cause methemoglobinemia and form reactive oxygen species. It is not clear whether they share the same chemical mechanism of methemoglobinemia as 5-HPQ. However, the great ability of the *N*-hydroxyl and quinone-imine derivatives to capture an electron suggests that they should be able to participate in redox reactions by transferring electrons. It was indeed found²⁰ that the quinone-imine derivative is able to react with the ferredoxin:NADP⁺ oxidoreductase and form hydrogen peroxide and hydroxyl radical. The possibility that the radical anions of the *N*-hydroxyl and quinone-imine derivatives are involved in oxidizing hemoglobin should be noted in future studies.

4. Conclusions

In the present work, we studied the electron affinities of PQ and several of its metabolites using a DFT method. We found that in the gas phase the substituents –CH₃, –OH and –OCH₃ at the 5-position do not significantly affect the electron affinities. In contrast, –Ph, –OPh and –CHO are all able to increase the adiabatic electron affinities (AEAs). However, except for –CHO all the other 5-position substituted PQs have negative or only slightly positive vertical electron affinities (VEAs), suggesting that they may not have sufficient lifetime to form stable covalently bound radical anions in the gas phase. In addition to –CHO, it is very likely that other electron-withdrawing groups at the 5-position will have a similar effect of increasing the AEA and having positive VEA and VDE. Thus, a strong electron-withdrawing group is needed at this position in order to make the PQ derivatives form stable radical anions. Other approaches to increase the electron capture ability of PQ in the gas phase include the use of an *N*-hydroxyl substituent at the 8-position and the formation of the quinone-imine derivative, as suggested by the significantly higher AEAs and positive VEAs of those metabolites.

In aqueous solution, all the molecules considered in this study have significantly larger AEAs than in the gas phase. In addition, all the VEAs are positive in solution, suggesting

that these molecules should be able to form stable radical anions in aqueous solution. Similarly as in the gas phase, the derivatives with an electron-withdrawing group at the 5-position, *N*-hydroxyl at the 8-position or the quinone-imine moiety have much larger AEAs than the other molecules we have considered.

The electron affinities calculated in this study provide insight into the toxicity of the 8-AQ antimalarial drugs. For example, the 5-HPQ metabolite cannot directly abstract an electron from Fe(II). As a result, our previously calculated mechanism²⁶ provides a more feasible explanation of the methemoglobinemia caused by this PQ metabolites. In addition, the strong ability of some of the metabolites, such as the *N*-hydroxyl and quinone-imine derivatives, to accept an electron should be noted. The formed radical anions may be able to get involved in oxidizing hemoglobin to methemoglobin and lead to erythrocyte oxidative stress by generation of hydrogen peroxide and superoxide radicals.

Supplementary Material

Refer to Web version on PubMed Central for supplementary material.

Acknowledgments

Computer time and resources from the Department of Medicinal Chemistry and the Mississippi Center for Supercomputer Research are greatly appreciated.

Funding sources: This project was partially supported by a grant to the University of Mississippi, W81-XWH-07-2-0095, awarded and administered by the U.S. Army Medical Research & Material Command (USAMRMC) and the Telemedicine & Advanced Technology Research Center (TATRC), at Fort Detrick, MD. The views, opinions and/or findings contained in this paper are those of the authors and do not necessarily reflect the views of the Department of Defense and should not be construed as an official DoD/Army position, policy or decision unless so designated by other documentation. LAW was partially supported by a U.S. Department of Agriculture, Agriculture Research Service, Cooperative Agreement # 58-6408-2-0009. This investigation was conducted in part in a facility constructed with support from Research Facilities Improvements Program (C06 RR-14503-01) from the NIH National Center for Research Resources.

References

1. Frey PA, Hegeman AD, Reed GH. Free radical mechanisms in enzymology. *Chem Rev.* 2006; 106:3302–3316. [PubMed: 16895329]
2. Ray SG, Daube SS, Naaman R. On the capturing of low-energy electrons by DNA. *Proc Natl Acad Sci USA.* 2005; 102:15–19. [PubMed: 15615850]
3. Gu JD, Xie YM, Schaefer HF. Electron attachment to DNA single strands: Gas phase and aqueous solution. *Nucleic Acids Res.* 2007; 35:5165–5172. [PubMed: 17660189]
4. Richardson NA, Gu J, Wang S, Xie Y, Schaefer HF. DNA nucleosides and their radical anions: Molecular structures and electron affinities. *J Am Chem Soc.* 2004; 126:4404–4411. [PubMed: 15053630]
5. Gu JD, Xie YM, Schaefer HF. Near 0 eV electrons attach to nucleotides. *J Am Chem Soc.* 2006; 128:1250–1252. [PubMed: 16433542]
6. Bao X, Wang J, Gu J, Leszczynski J. DNA strand breaks induced by near-zero-electronvolt electron attachment to pyrimidine nucleotides. *Proc Natl Acad Sci USA.* 2006; 103:5658–5663. [PubMed: 16585526]
7. Schyman P, Laaksonen A. On the effect of low-energy electron induced DNA strand break in aqueous solution: A theoretical study indicating guanine as a weak link in DNA. *J Am Chem Soc.* 2008; 130:12254–12255. [PubMed: 18715005]
8. Simons J. How do low-energy (0.1–2 eV) electrons cause DNA-strand breaks? *Acc Chem Res.* 2006; 39:772–779. [PubMed: 17042477]

9. Ptasinska S, Denifl S, Gohlke S, Scheier P, Illenberger E, Märk TD. Decomposition of thymidine by low-energy electrons: Implications for the molecular mechanisms of single-strand breaks in DNA. *Angew Chem Int Ed*. 2006; 45:1893–1896.
10. Kumar A, Sevilla MD. Role of excited states in low-energy electron (LEE) induced strand breaks in DNA model systems: Influence of aqueous environment. *ChemPhysChem*. 2009; 10:1426–1430. [PubMed: 19308972]
11. Llano J, Eriksson LA. Oxidation pathways of adenine and guanine in aqueous solution from first principles electrochemistry. *Phys Chem Chem Phys*. 2004; 6:4707–4713.
12. Huels MA, Hahndorf I, Illenberger E, Sanche L. Resonant dissociation of DNA bases by subionization electrons. *J Chem Phys*. 1998; 108:1309–1312.
13. Zheng Y, Cloutier P, Hunting DJ, Wagner JR, Sanche L. Glycosidic bond cleavage of thymidine by low-energy electrons. *J Am Chem Soc*. 2004; 126:1002–1003. [PubMed: 14746451]
14. Xie H, Wu R, Xia F, Cao Z. Effects of electron attachment on C5'-O5' and C1'-N1' bond cleavages of pyrimidine nucleotides: A theoretical study. *J Comput Chem*. 2008; 29:2025–2032. [PubMed: 18432616]
15. Gu JD, Xie YM, Schaefer HF. Glycosidic bond cleavage of pyrimidine nucleosides by low-energy electrons: A theoretical rationale. *J Am Chem Soc*. 2005; 127:1053–1057. [PubMed: 15656644]
16. Frischer H, Mellovitz RL, Ahmad T, Nora MV. The conversion of primaquine into primaquine-aldehyde, primaquine-alcohol, and carboxyprimaquine, a major plasma metabolite. *J Lab Clin Med*. 1991; 117:468–476. [PubMed: 2045714]
17. Constantino L, Paixao P, Moreira R, Portela MJ, Do Rosario VE, Iley J. Metabolism of primaquine by liver homogenate fractions. Evidence for monoamine oxidase and cytochrome P450 involvement in the oxidative deamination of primaquine to carboxyprimaquine. *Exp Toxic Pathol*. 1999; 51:299–303.
18. Bowman ZS, Oatis JE, Whelan JL, Jollow DJ, McMillan DC. Primaquine-induced hemolytic anemia: Susceptibility of normal versus glutathione-depleted rat erythrocytes to 5-hydroxyprimaquine. *J Pharmacol Exp Ther*. 2004; 309:79–85. [PubMed: 14724225]
19. Bowman ZS, Jollow DJ, McMillan DC. Primaquine-induced hemolytic anemia: Role of splenic macrophages in the fate of 5-hydroxyprimaquine-treated rat erythrocytes. *J Pharmacol Exp Ther*. 2005; 315:980–986. [PubMed: 16099929]
20. Vazquez-Vivar J, Augusto O. Hydroxylated metabolites of the antimalarial drug primaquine. Oxidation and redox cycling. *J Biol Chem*. 1992; 267:6848–6854. [PubMed: 1313024]
21. Bolchoz LJC, Budinsky RA, McMillan DC, Jollow DJ. Primaquine-induced hemolytic anemia: Formation and hemotoxicity of the arylhydroxylamine metabolite 6-methoxy-8-hydroxylaminoquinoline. *J Pharmacol Exp Ther*. 2001; 297:509–515. [PubMed: 11303037]
22. Bolchoz LJC, Gelasco AK, Jollow DJ, McMillan DC. Primaquine-induced hemolytic anemia: Formation of free radicals in rat erythrocytes exposed to 6-methoxy-8-hydroxylaminoquinoline. *J Pharmacol Exp Ther*. 2002; 303:1121–1129. [PubMed: 12438535]
23. Vale N, Moreira R, Gomes P. Primaquine revisited six decades after its discovery. *Eur J Med Chem*. 2009; 44:937–953. [PubMed: 18930565]
24. Srivastava P, Singh S, Jain GK, Puri SK, Pandey VC. A simple and rapid evaluation of methemoglobin toxicity of 8-aminoquinolines and related compounds. *Ecotoxicol Environ Saf*. 2000; 45:236–239. [PubMed: 10702341]
25. Suryanaryana V, Meenakshi J, Kirandeep K, Premanand P, Sanjay RP, Rahul J. Recent advances in antimalarial drug development. *Med Res Rev*. 2007; 27:65–107. [PubMed: 16700012]
26. Liu H, Walker LA, Nanayakkara NPD, Doerksen RJ. Methemoglobinemia caused by 8-aminoquinoline drugs: DFT calculations suggest an analogy to H4B's role in nitric oxide synthase. *J Am Chem Soc*. 2011; 133:1172–1175. [PubMed: 21244096]
27. Rienstra-Kiracofe JC, Tschumper GS, Schaefer HF, Nandi S, Ellison GB. Atomic and molecular electron affinities: Photoelectron experiments and theoretical computations. *Chem Rev*. 2002; 102:231–282. [PubMed: 11782134]
28. Gu J, Xie Y, Schaefer HF. Guanine nucleotides: Base-centered and phosphate-centered valence-bound radical anions in aqueous solution. *J Phys Chem B*. 2009; 114:1221–1224. [PubMed: 20039616]

29. Gu JA, Xie YM, Schaefer HF. Understanding electron attachment to the DNA double helix: The thymidine monophosphate-adenine pair in the gas phase and aqueous solution. *J Phys Chem B*. 2006; 110:19696–19703. [PubMed: 17004839]
30. Gu JA, Xie YM, Schaefer HF. Electron attachment to nucleotides in aqueous solution. *ChemPhysChem*. 2006; 7:1885–1887. [PubMed: 16915601]
31. Kim S, Meehan T, Schaefer HF. Hydrogen-atom abstraction from the adenine-uracil base pair. *J Phys Chem A*. 2007; 111:6806–6812. [PubMed: 17388361]
32. Kim S, Schaefer HF. Effects of microsolvation on the adenine-uracil base pair and its radical anion: Adenine-uracil mono- and dihydrates. *J Phys Chem A*. 2007; 111:10381–10389. [PubMed: 17705454]
33. Lind MC, Richardson NA, Wheeler SE, Schaefer HF. Hydrogen-abstracted adenine-thymine radicals with interesting transferable properties. *J Phys Chem B*. 2007; 111:5525–5530. [PubMed: 17458994]
34. Zhang JD, Schaefer HF. Molecular structures and energetics associated with hydrogen atom addition to the guanine-cytosine base pair. *J Chem Theory Comput*. 2007; 3:115–126.
35. Zhang JD, Xie Y, Schaefer HF. Successive attachment of electrons to protonated guanine: (G+H) radicals and (G+H)[−] anions. *J Phys Chem A*. 2006; 110:12010–12016. [PubMed: 17064190]
36. Frisch, MJ.; Trucks, GW.; Schlegel, HB.; Scuseria, GE.; Robb, MA.; Cheeseman, JR.; Scalmani, G.; Barone, V.; Mennucci, B.; Petersson, GA.; Nakatsuji, H.; Caricato, M.; Li, X.; Hratchian, HP.; Izmaylov, AF.; Bloino, J.; Zheng, G.; Sonnenberg, JL.; Hada, M.; Ehara, M.; Toyota, K.; Fukuda, R.; Hasegawa, J.; Ishida, M.; Nakajima, T.; Honda, Y.; Kitao, O.; Nakai, H.; Vreven, T.; Montgomery, JJA.; Peralta, JE.; Ogliaro, F.; Bearpark, M.; Heyd, JJ.; Brothers, E.; Kudin, KN.; Staroverov, VN.; Kobayashi, R.; Normand, J.; Raghavachari, K.; Rendell, A.; Burant, JC.; Iyengar, SS.; Tomasi, J.; Cossi, M.; Rega, N.; Millam, JM.; Klene, M.; Knox, JE.; Cross, JB.; Bakken, V.; Adamo, C.; Jaramillo, J.; Gomperts, R.; Stratmann, RE.; Yazyev, O.; Austin, AJ.; Cammi, R.; Pomelli, C.; Ochterski, JW.; Martin, RL.; Morokuma, K.; Zakrzewski, VG.; Voth, GA.; Salvador, P.; Dannenberg, JJ.; Dapprich, S.; Daniels, AD.; Farkas, O.; Foresman, JB.; Ortiz, JV.; Cioslowski, J.; Fox, DJ. Gaussian 09. Gaussian, Inc.; Wallingford CT:
37. Becke AD. A new mixing of Hartree-Fock and local density-functional theories. *J Chem Phys*. 1993; 98:1372–1377.
38. Becke AD. Density-functional thermochemistry. III. The role of exact exchange. *J Chem Phys*. 1993; 98:5648–5652.
39. Lee C, Yang W, Parr RG. Development of the colle-salvetti correlation-energy formula into a functional of the electron density. *Phys Rev B*. 1988; 37:785–789.
40. Li X, Cai Z, Sevilla MD. DFT calculations of the electron affinities of nucleic acid bases: Dealing with negative electron affinities. *J Phys Chem A*. 2002; 106:1596–1603.
41. Sommerfeld T. Intramolecular electron transfer from dipole-bound to valence orbitals: Uracil and 5-chlorouracil. *J Phys Chem A*. 2004; 108:9150–9154.
42. Nanayakkara NPD, Ager AL Jr, Bartlett MS, Yardley V, Croft SL, Khan IA, McChesney JD, Walker LA. Antiparasitic activities and toxicities of individual enantiomers of the 8-aminoquinoline 8-[(4-amino-1-methylbutyl)amino]-6-methoxy-4-methyl-5-[3,4-dichlorophenoxy]quinoline succinate. *Antimicrob Agents Chemother*. 2008; 52:2130–2137. [PubMed: 18378716]
43. Li X, Cai Z, Sevilla MD. Energetics of the radical ions of the AT and AU base pairs: A density functional theory (DFT) study. *J Phys Chem A*. 2002; 106:9345–9351.
44. Vásquez-Vivar J, Augusto O. Oxidative activity of primaquine metabolites on rat erythrocytes in vitro and in vivo. *Biochem Pharmacol*. 1994; 47:309–316. [PubMed: 8304975]

Abbreviations

5-HPQ	5-hydroxyprimaquine
5,6-HPQ	5,6-dihydroxyprimaquine

8-AQ	8-aminoquinoline
AEA	adiabatic electron affinity
DFT	density functional theory
FAD	flavin adenine dinucleotide
G6PD	glucose-6-phosphate dehydrogenase
IEFPCM	integral equation formalism polarizable continuum model
MAQ	6-methoxy-8-aminoquinoline
MAQ-NOH	6-methoxy-8-(<i>N</i> -hydroxy)aminoquinoline
PQ	primaquine
SOMO	singly occupied molecule orbital
VDE	vertical detachment energy
VEA	vertical electron affinity
ZPVE	zero-point vibrational energy

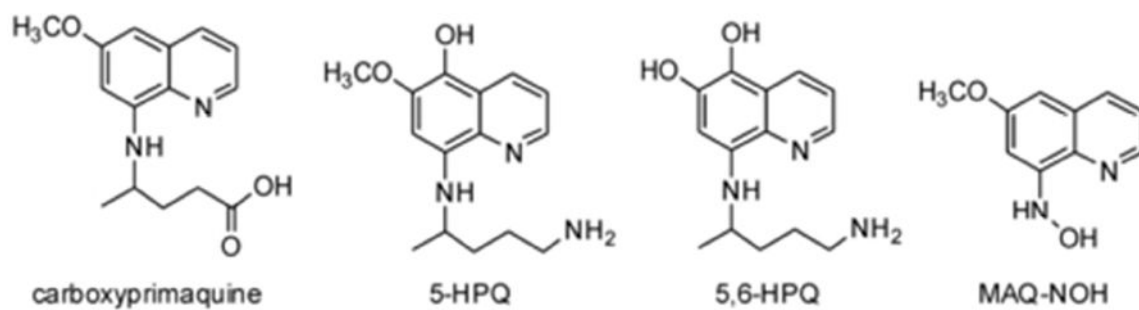


Figure 1.
A schematic illustration of the structures of selected primaquine metabolites.

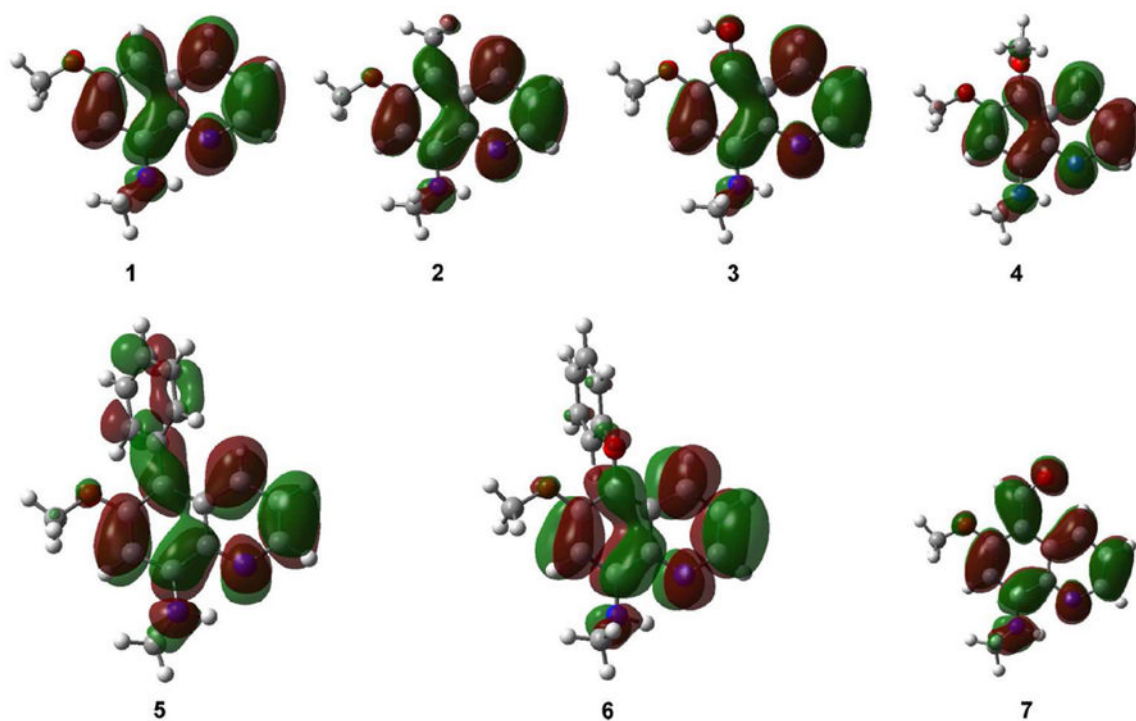


Figure 2.
The SOMO (singly-occupied molecular orbital) of the radical anions of **1–7**.

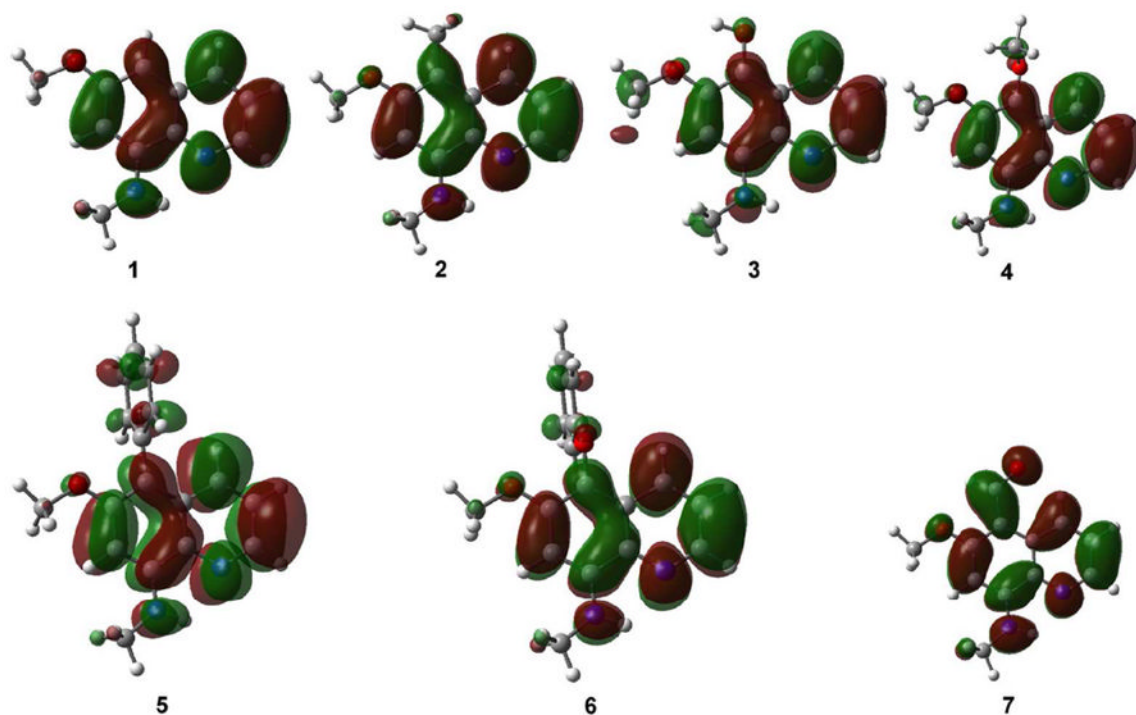


Figure 3.
The SOMO of the vertically-attached electron radical anions of **1–7**.

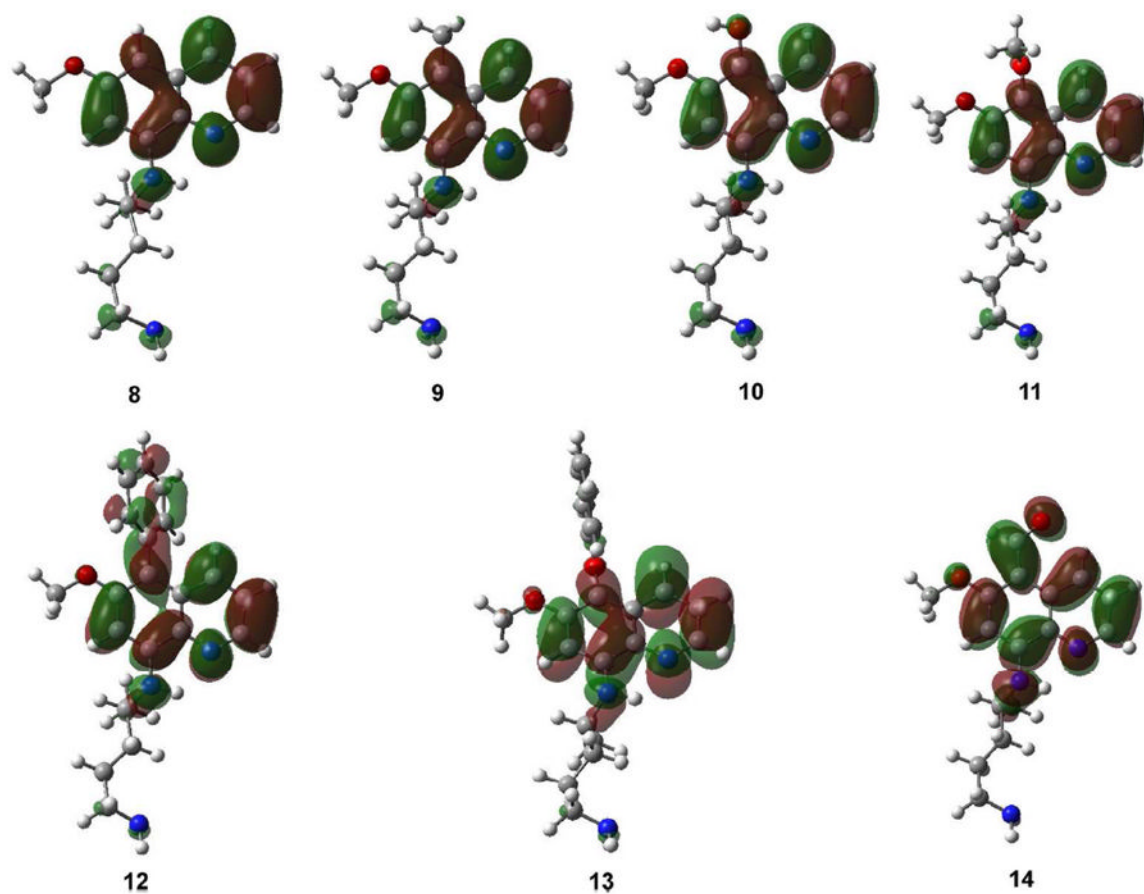


Figure 4.
The SOMO of the radical anions of 8–14.

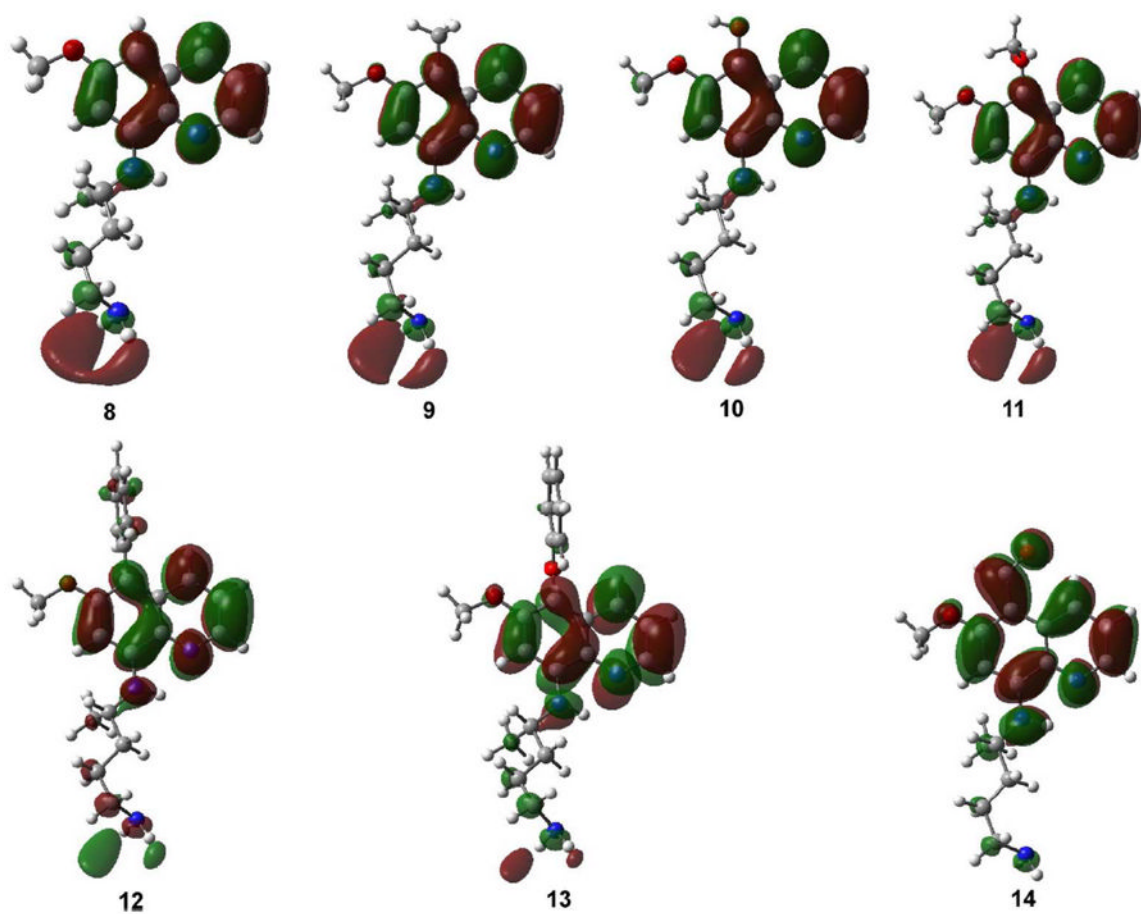


Figure 5.
The SOMO of the vertically-attached electron radical anions of **8–14**.

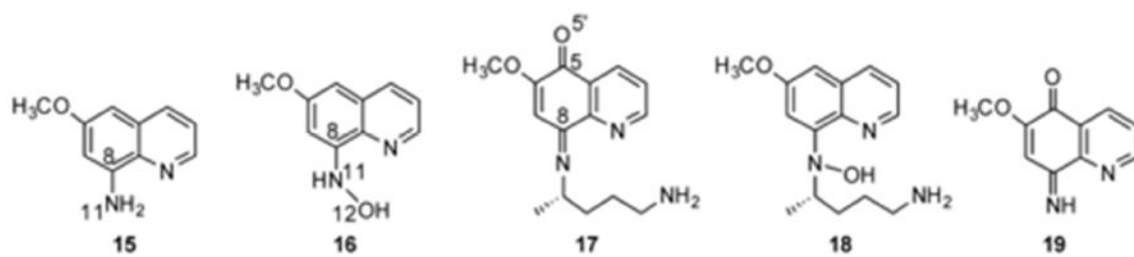


Figure 6.
A schematic illustration of **15–19**.

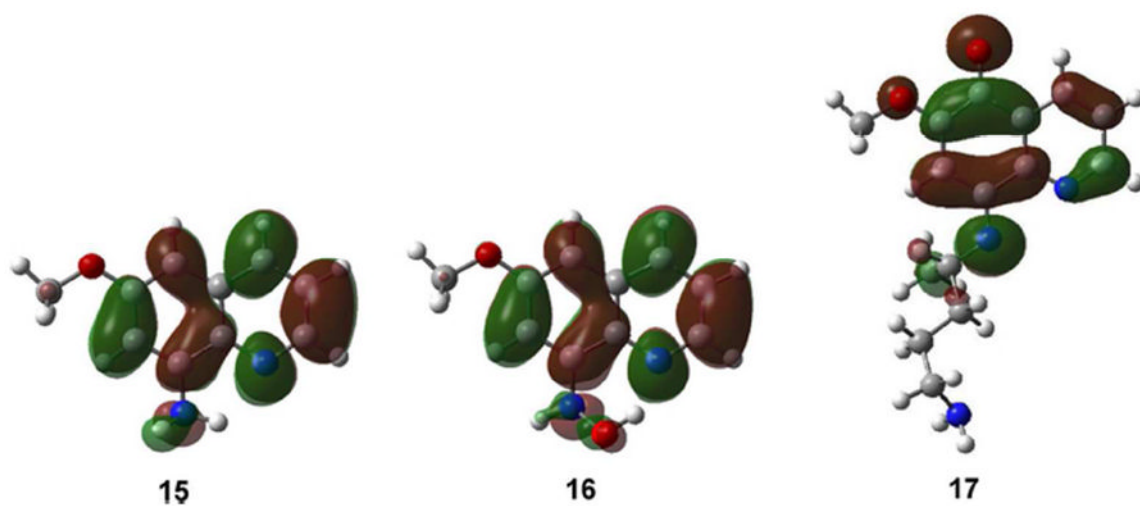


Figure 7.
The SOMO of the radical anions of **15–17**.

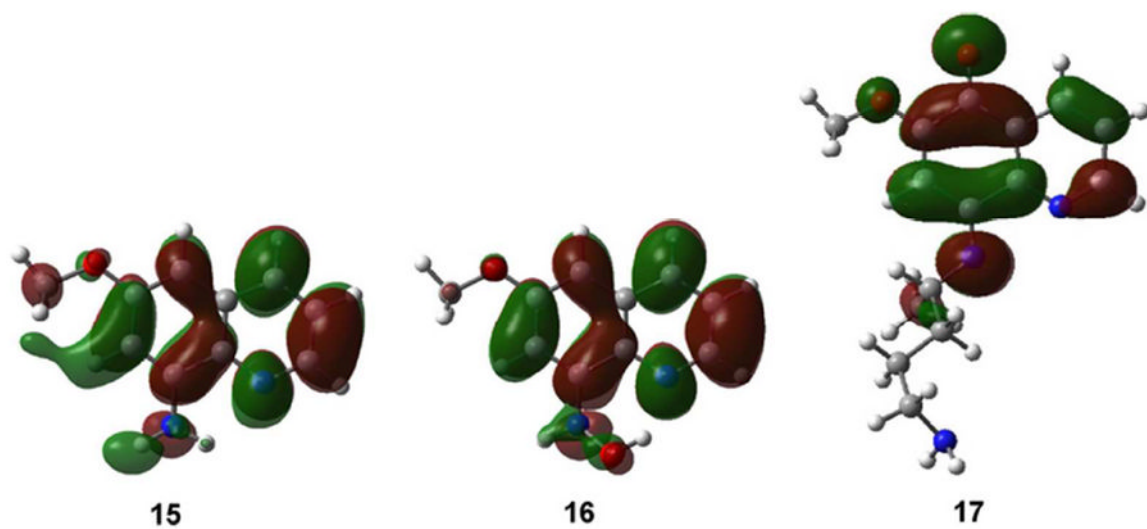


Figure 8.
The SOMO of the vertically-attached electron radical anions of **15–17**.

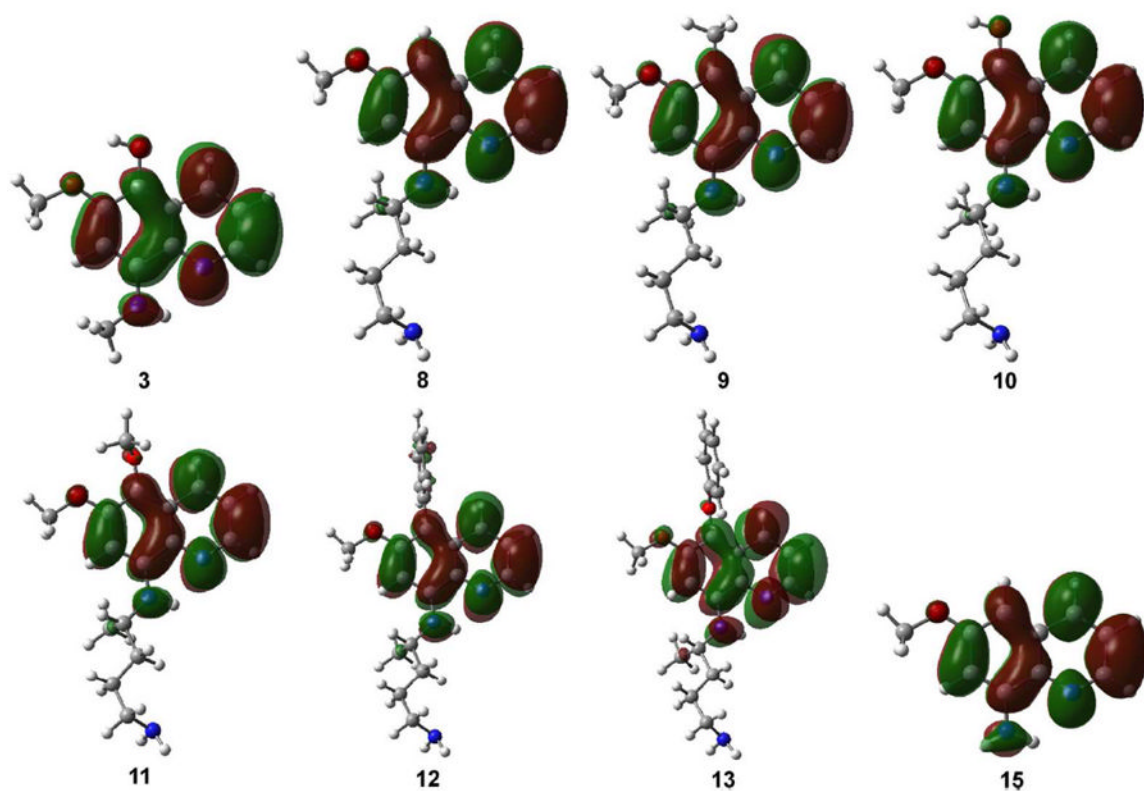
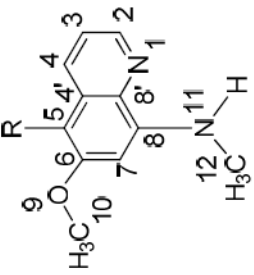


Figure 9.
The SOMO of the vertically-attached electron radical anions of **3**, **8–13** and **19** in solution.

The key bond lengths (Å) and dihedral angles (°) of model 8-aminoquinoline molecules, with a methyl substituent on the 8-amino group, in the neutral and radical anion (in parentheses) forms. Six substituents, $-\text{CH}_3$, $-\text{OH}$, $-\text{OCH}_3$, $-\text{Ph}$, $-\text{OPh}$ and $-\text{CHO}$, were chosen at the 5-position.

Table 1



	$-\text{H}$ (1)	$-\text{CH}_3$ (2)	$-\text{OH}$ (3)	$-\text{OCH}_3$ (4)	$-\text{Ph}$ (5)	$-\text{OPh}$ (6)	$-\text{CHO}$ (7)
N1-C2	1.32 (1.35)	1.32 (1.35)	1.32 (1.36)	1.32 (1.36)	1.32 (1.35)	1.32 (1.35)	1.32 (1.34)
C2-C3	1.42 (1.40)	1.42 (1.39)	1.42 (1.39)	1.42 (1.39)	1.42 (1.39)	1.42 (1.39)	1.41 (1.40)
C3-C4	1.38 (1.42)	1.38 (1.42)	1.38 (1.42)	1.38 (1.42)	1.38 (1.42)	1.38 (1.42)	1.38 (1.41)
C4-C4'	1.42 (1.42)	1.43 (1.43)	1.42 (1.42)	1.42 (1.42)	1.43 (1.42)	1.42 (1.42)	1.43 (1.41)
C4'-C5	1.42 (1.42)	1.43 (1.43)	1.42 (1.42)	1.42 (1.42)	1.43 (1.45)	1.42 (1.42)	1.44 (1.46)
C5-C6	1.39 (1.40)	1.40 (1.41)	1.39 (1.40)	1.40 (1.41)	1.40 (1.42)	1.39 (1.41)	1.42 (1.44)
C5-R ^a	1.09 (1.09)	1.51 (1.51)	1.38 (1.40)	1.38 (1.40)	1.50 (1.48)	1.39 (1.41)	1.47 (1.44)
C6-C7	1.42 (1.40)	1.42 (1.40)	1.42 (1.40)	1.42 (1.40)	1.42 (1.40)	1.42 (1.40)	1.41 (1.39)
C7-C8	1.40 (1.42)	1.39 (1.42)	1.40 (1.41)	1.40 (1.42)	1.40 (1.42)	1.40 (1.42)	1.40 (1.42)
C8-C8'	1.45 (1.42)	1.44 (1.42)	1.44 (1.42)	1.44 (1.42)	1.45 (1.42)	1.45 (1.42)	1.45 (1.42)
C4'-C8'	1.43 (1.45)	1.43 (1.45)	1.43 (1.45)	1.43 (1.45)	1.43 (1.45)	1.43 (1.45)	1.42 (1.45)
C8-N11	1.37 (1.42)	1.37 (1.42)	1.38 (1.42)	1.37 (1.42)	1.37 (1.42)	1.37 (1.42)	1.36 (1.42)
N11-C12	1.44 (1.46)	1.44 (1.46)	1.44 (1.46)	1.44 (1.46)	1.44 (1.46)	1.44 (1.46)	1.45 (1.46)
C6-O9	1.37 (1.40)	1.38 (1.40)	1.38 (1.40)	1.37 (1.39)	1.37 (1.39)	1.36 (1.39)	1.36 (1.39)
O9-C10	1.42 (1.41)	1.42 (1.41)	1.42 (1.41)	1.42 (1.41)	1.42 (1.41)	1.42 (1.41)	1.42 (1.41)
C8'-C8-N11-C12	180 (136)	180 (135)	168 (131)	-172 (-133)	180 (-136)	179 (136)	180 (137)

^aR is the atom directly connected to C5.

Table 2

The calculated adiabatic electron affinities (AEAs), vertical electron affinities (VEAs) and vertical detachment energies (VDEs) (eV) of **1–14**.

R	AEA^a	VEA	VDE	AEA^a	VEA	VDE
1 -H	0.12	-0.25	0.24	8 0.14	-0.07	0.15
2 -CH ₃	0.13	-0.23	0.25	9 0.15	-0.06	0.16
3 -OH	0.10	-0.16	0.22	10 0.13	-0.08	0.14
4 -OCH ₃	0.16	-0.21	0.30	11 0.18	-0.05	0.20
5 -Ph	0.27	-0.13	0.41	12 0.27	-0.01	0.35
6 -OPh	0.34	-0.02	0.48	13 0.35	0.08	0.43
7 -CHO	0.72	0.38	0.93	14 0.70	0.38	0.90

^a AEAs are reported with ZPVE corrections.

Table 3

The key bond lengths (Å) and dihedral angles (°) of 8-aminoquinoline molecules, with the complete alkyl-amine chain, connected to the 8-amino group in the neutral and radical anion (in parentheses) forms. Six substituents, -CH₃, -OH, -OCH₃, -Ph, -OPh and -CHO, were chosen at the 5-position.

	R ^a					
	-H (8)	-CH ₃ (9)	-OH (10)	-OCH ₃ (11)	-Ph (12)	-OPh (13)
N1-C2	1.32 (1.35)	1.32 (1.35)	1.32 (1.35)	1.32 (1.35)	1.32 (1.34)	1.32 (1.35)
C2-C3	1.42 (1.40)	1.42 (1.40)	1.42 (1.40)	1.42 (1.40)	1.42 (1.40)	1.42 (1.39)
C3-C4	1.38 (1.41)	1.38 (1.41)	1.38 (1.41)	1.38 (1.41)	1.38 (1.41)	1.38 (1.42)
C4-C4'	1.42 (1.42)	1.43 (1.43)	1.42 (1.42)	1.42 (1.42)	1.43 (1.42)	1.42 (1.42)
C4'-C5	1.42 (1.42)	1.43 (1.43)	1.42 (1.42)	1.42 (1.42)	1.43 (1.44)	1.42 (1.42)
C5-C6	1.39 (1.40)	1.40 (1.40)	1.39 (1.40)	1.40 (1.40)	1.40 (1.42)	1.39 (1.41)
C5-R ^a	1.09 (1.09)	1.51 (1.51)	1.38 (1.39)	1.38 (1.40)	1.49 (1.48)	1.39 (1.41)
C6-C7	1.42 (1.41)	1.42 (1.41)	1.42 (1.41)	1.42 (1.41)	1.42 (1.40)	1.42 (1.40)
C7-C8	1.40 (1.41)	1.39 (1.41)	1.40 (1.41)	1.40 (1.41)	1.40 (1.41)	1.40 (1.42)
C8-C8'	1.45 (1.43)	1.45 (1.43)	1.44 (1.43)	1.44 (1.43)	1.45 (1.42)	1.45 (1.42)
C4'-C8'	1.43 (1.44)	1.43 (1.44)	1.43 (1.44)	1.43 (1.44)	1.43 (1.45)	1.43 (1.45)
C8-N11	1.37 (1.40)	1.37 (1.41)	1.38 (1.41)	1.37 (1.41)	1.37 (1.41)	1.37 (1.42)
N11-Cl2	1.46 (1.46)	1.46 (1.46)	1.46 (1.46)	1.46 (1.46)	1.46 (1.46)	1.44 (1.46)
C6-O9	1.37 (1.39)	1.38 (1.40)	1.38 (1.40)	1.39 (1.39)	1.37 (1.39)	1.36 (1.39)
O9-C10	1.42 (1.41)	1.42 (1.41)	1.42 (1.41)	1.42 (1.41)	1.42 (1.41)	1.42 (1.41)
C8'-C8-N11-C12	-170 (-148)	-168 (-146)	-164 (-143)	-166 (-145)	-170 (-139)	179 (136)
						-176 (-135)

^aR is the atom directly connected to C5.

Table 4

The calculated adiabatic electron affinities (AEAs), vertical electron affinities (VEAs) and vertical detachment energies (VDEs) (eV) of **15–19**.

	AEA ^a	VEA	VDE
15	0.19	−0.11	0.26
16	0.56	0.23	0.62
17	1.63	1.28	1.79
18	0.48	0.15	0.55
19	1.69	1.39	1.84

^aAEAs are reported with ZPVE corrections.

Table 5

The calculated adiabatic electron affinities (AEAs), vertical electron affinities (VEAs) and vertical detachment energies (VDEs) (eV) of **1-14** in aqueous solution.

R	AEA	VEA	VDE	AEA	VEA	VDE
1 -H	2.08 ^a	1.76	2.19	8 2.07 ^a	1.76	2.06
1^b -H	2.07 ^c	1.77	2.16	8^b 2.08 ^c	1.77	2.15
2 -CH ₃	2.06 ^a	1.74	2.16	9 2.06 ^a	1.75	2.04
3 -OH	2.09 ^a	1.79	2.19	10 2.08 ^a	1.78	2.07
4 -OCH ₃	2.10 ^a	1.78	2.22	11 2.10 ^a	1.78	2.10
5 -Ph	2.06 ^a	1.78	2.21	12 2.08 ^a	1.78	2.15
6 -OPh	2.16 ^a	1.85	2.30	13 2.19 ^a	1.86	2.24
7 -CHO	2.55 ^a	2.26	2.76	14 2.56 ^a	2.25	2.45

^aCorrected with ZPVEs obtained from gas-phase frequency calculations.

^bBased on the optimized geometries in solution.

^cCorrected with ZPVEs obtained from solution frequency calculations.

Table 6

The calculated adiabatic electron affinities (AEAs), vertical electron affinities (VEAs) and vertical detachment energies (VDEs) (eV) of **15-19** in aqueous solution.

	AEA ^a	VEA	VDE
15	2.14	1.85	2.21
16	2.43	2.09	2.46
17	3.56	3.21	3.69
18	2.37	2.00	2.40
19	3.65	3.34	3.79

^aCorrected with ZPVEs obtained from gas-phase frequency calculations.